Regional and temporal variations affect the accuracy of variant-specific SARS-CoV-2 PCR assays

Chamteut Oh[1,*], Palash Sashittal[2,*], Aijia Zhou[1], Leyi Wang[3], Mohammed El-Kebir[2], Thanh H. Nguyen[1,4]

[*]*Equal contribution*
Corresponding authors: Than H. Nguyen (thn@illinois.edu) and Mohammed El-Kebir (melkebir@illinois.edu)

1) Department of Civil and Environmental Engineering, University of Illinois at Urbana-Champaign, United States
2) Department of Computer Science, University of Illinois at Urbana-Champaign, United States
3) Veterinary Diagnostic Laboratory and Department of Veterinary Clinical Medicine, University of Illinois at Urbana-Champaign, United States
4) Institute of Genomic Biology, University of Illinois at Urbana-Champaign, United States

Abstract

Monitoring the prevalence of SARS-CoV-2 variants is necessary to make informed public health decisions during the COVID-19 pandemic. PCR assays have received global attention, facilitating rapid understanding of variant dynamics because they are more accessible and scalable than genome sequencing. However, as PCR assays target only a few mutations, their accuracy could be compromised when these mutations are not exclusive to target variants. Here we show how to design variant-specific PCR assays with high sensitivity and specificity across different geographical regions by incorporating sequences deposited in the GISAID database. Furthermore, we demonstrate that several previously developed PCR assays have decreased accuracy outside their study areas. We introduce `PRIMES`, an algorithm that enables the design of reliable PCR assays, as demonstrated in our experiments that enabled tracking of dominant SARS-CoV-2 variants in local sewage samples. Our findings will contribute to improving PCR assays for SARS-CoV-2 variant surveillance.

Key words: PCR assays; SARS-CoV-2 variants; *in silico* analysis; `PRIMES`; Wastewater-based epidemiology.

Introduction

SARS-CoV-2 has had an unprecedented impact on public health globally. However, despite the availability of vaccines, emerging new variants, which may have better infectivity, transmissibility, and immune evasion, threaten global public health again[1,2]. Monitoring the introduction and prevalence of variants of concern (VOCs) and variants of interest (VOIs) in a community can help the local authorities make informed decisions regarding public health[3–5]. In particular, wastewater-based epidemiology (WBE) has been applied across the globe to monitor SARS-CoV-2 circulating in a community[6–9]. WBE could complement clinical diagnosis because WBE allows health authorities to monitor transmission levels in communities, including asymptomatic patients, without requiring excessive resources[10].

Although sequencing is considered the gold standard to identify SARS-CoV-2 lineages, PCR assays have attracted global attention for variant detection due to several advantages[11]. First, PCR is a more accessible tool because the instruments and reagents are more affordable. Second, PCR is more scalable because it can analyze dozens or hundreds of samples in only a few hours, while sequencing takes a much longer time (>12 hours)[12]. Third, PCR is more robust to sewage samples that have low concentrations of SARS-CoV-2 genomes and contain different types of impurities[13]. These advantages are beneficial to ramp up capacity for SARS-CoV-2 surveillance and facilitate deployment in regions where there is a lack of access to sequencing facilities to initiate their variant monitoring systems.

PCR assays are composed of about 20 to 30 base pair long primers or probes designed to detect single or multiple loci that characterize a target variant. Importantly, PCR assays can only examine less than 100 bp long sequences, while sequencing produces reads that span longer genome regions (> 1000 bp). Meanwhile, each variant or sub-lineage of SARS-CoV-2 is defined

by a group of different mutations located throughout the entire genome. Therefore, distinct variants may have the same mutations, reducing specificity when used in PCR assays[14].

In this study, we introduce a computational tool, PRIMES (PRIMer Efficacy Sleuth), that can be used to analyze sequences available in open source databases such as GISAID[15,16], to predict the sensitivity and specificity of a PCR assay to detect specific pathogen lineages of interest. Moreover, for a given set of mutations characterizing the target variant, PRIMES can also identify a subset of variant-specific mutations for designing PCR assays with high specificity and sensitivity. Using PRIMES, we show multiple examples of previous PCR assays[13,17,18] that were successfully applied to certain study areas might not work for other regions (**Fig. 1**). We also demonstrate that the PCR assays designed using PRIMES successfully identify the dominant lineages in sewage samples from Champaign County, IL, USA. We conclude that PCR assays ought to be designed or modified considering regional and temporal variations and that *in silico* analyses using open source databases can address the weaknesses of PCR assays. These findings will allow PCR assays to be applied more reliably for SARS-CoV-2 surveillance.

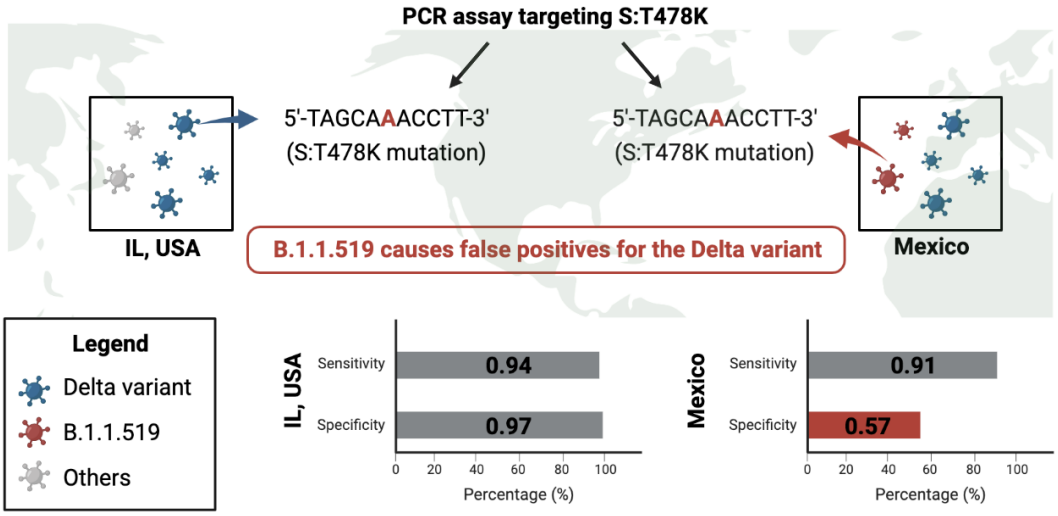

Fig. 1. Study overview.

Results

Analysis and design of PCR assays using PRIMES

As new variants of SARS-CoV-2 emerge and fade away throughout the world, a number of different lineages (1340 lineages as of August 2021) have been reported[19]. Due to the evolutionary relationship of these lineages, they often share characteristic mutations. As such, PCR assays targeting only a few mutations (typically 1-3 mutations) have difficulty detecting samples from a specific lineage of interest with high specificity and sensitivity. In addition, while most lineages are limited to where they emerged, outbreaks of some lineages occasionally spread across the borders and become global concerns (such as variants of concern (VOCs) and variants of interest (VOIs)). Thus, regional and temporal differences in variant dynamics have to be considered for PCR assays.

The most widely used computational tool for assigning lineages to SARS-CoV-2 genomes is the Phylogenetic Assignment of Named Global Outbreak Lineages (Pangolin, https://pangolin.cog-uk.io/). Pangolin is a lineage designation pipeline that takes a FASTA file as input, containing one or more query sequences. Each query sequence is first aligned to the SARS-CoV-2 reference genome (Wuhan-Hu-1, NC_045512.2) using minimap2 v2.17[20]. After trimming the non-coding regions in the 5' and 3' ends of the aligned sequences, they are assigned to the most likely lineage out of all currently designated lineages using an underlying machine learning model referred to as PangoLEARN. The current version of PangoLEARN is a decision tree that is trained on data from GISAID that was manually curated with lineages.

By considering the lineage designation of Pangolin as ground truth, we perform an *in silico* analysis of the efficacy of PCR assays using `PRIMES` (available at https://github.com/elkebir-group/primer-analysis). Specifically, we search for the probing sequence (containing a mutation

100 targeted by the PCR assay) in each GISAID sequence and then estimate the overall specificity and
101 sensitivity of the PCR assay. While this information is crucial in its own right, it can also be used
102 to design lineage-specific PCR assays. Specifically, for a lineage of interest and a set of
103 characteristic mutations, we use PRIMES to identify the set of mutations that should be targeted
104 by PCR assays to get high specificity and sensitivity. We employ this approach to design PCR
105 assays to detect the presence SARS-CoV-2 of both Alpha (e.g., B.1.1.7) and Delta (e.g., B.1.617.2)
106 variants in sewage samples.
107

108 **Analysis of previously developed PCR assays**

109 Here, we use PRIMES to analyze the efficacy of previously developed PCR assays targeting
110 specific Spike (S) protein mutations in the SARS-CoV-2 genome. Recall that sensitivity and
111 specificity are defined as follows.
112

113 $$Sensitivity = \frac{True\ positive}{True\ positive + False\ negative} \quad \text{(Eq. 1)}$$

114 $$Specificity = \frac{True\ negative}{True\ negative + False\ positive} \quad \text{(Eq. 2)}$$

115

116 where true positive indicates the number of virus sequences that include the primer sequences and
117 also belong to the lineage of interest. False negative is the number of virus sequences that do not
118 include the primer sequences but belong to the lineage of interest. True negative is the number of
119 virus sequences that do not include the primer sequences and do not belong to the lineage of
120 interest as well. Finally, false positive indicates the number of virus sequences that include the
121 primer sequences but belong to the lineage of interest. Strikingly, our analysis shows that several

122 previously developed PCR assays would not be as accurate for samples collected from locations
123 and periods beyond those included in the original study.

124 First, we focus on analyzing PCR assays targeting S:Δ69/70 to detect the Alpha
125 variant[13,18,21]. These PCR assays were verified with synthetic RNA controls and local sewage
126 samples from Israel. Then, we simulated the application of these assays to sequences deposited in
127 GISAID for Israel (n=13932 from January 2021 to October 2021). **Fig. 2a** shows that the Alpha
128 variant was dominant (most prevalent variant) from January 2021 until May 2021, after which
129 most samples were from other lineages. `PRIMES` predicts that the PCR assays targeting S:Δ69/70[18]
130 correctly assigned GISAID samples to the Alpha variants with a sensitivity of 0.95 and a specificity
131 of 0.93. This finding can be attributed to the observation that the target mutations of these PCR
132 assays, S:Δ69/70, is mostly exclusive to the Alpha variant in Israel, where this PCR assay was
133 developed. However, although S:Δ69/70 was once a key mutation for the Alpha variant (B.1.1.7
134 first reported in February 2020), B.1.258.17 (first reported in August 2020) and B.1.620 (first
135 reported in February 2021) and more lineages are also known to have the same mutation. Although
136 these SARS-CoV-2 lineages are not significant in Israel (29/13932), they have significant
137 prevalence in certain regions at some points in time due to local outbreaks. For example, the
138 B.1.258.17 lineage accounted for 21.8% of all the sequences on GISAID from Slovenia for the
139 period between January 2021 to October 2021.

140 While this PCR assay targeting S:Δ69/70 was only applied to wastewater samples from
141 Israel in the previous study[18], we can use `PRIMES` to predict the sensitivity and specificity of this
142 PCR assay on GISAID samples from any other region. **Fig. 2b** shows our analysis on samples
143 from Slovenia (n=25528, from January 2021 to October 2021) where the prevalence of lineage
144 B.1.258.17 was significant until May 2021 and dominating in January 2021 and February 2021.

On the other hand, Alpha variant has less than 10% prevalence in January 2021 and February 2021. However, our analysis of the PCR assays shows that the Alpha would have been dominant from January 2021 until June 2021. This error came from the fact that these assays would have incorrectly assigned genomes belonging to the B.1.258 and B.1.258.17 lineages to the Alpha variant. The false positives for the Alpha variant continued until June 2021 the B.1.258.17 lineage fades out. Thus, while the estimated sensitivity of the assay for the Alpha variant in Slovenia is 0.89, the specificity is estimated to be only 0.68. We also found that PCR assays targeting S:Δ69/70 could lead to significant amounts of false positives when applied to samples from the Central African Republic (**Fig. 2c** shows that the estimated specificity is only 0.46 due to samples from B.1.620), Republic of Congo (**Fig. 2d** shows that the estimated specificity is only 0.64 due to B.1.620 and B.1.631).

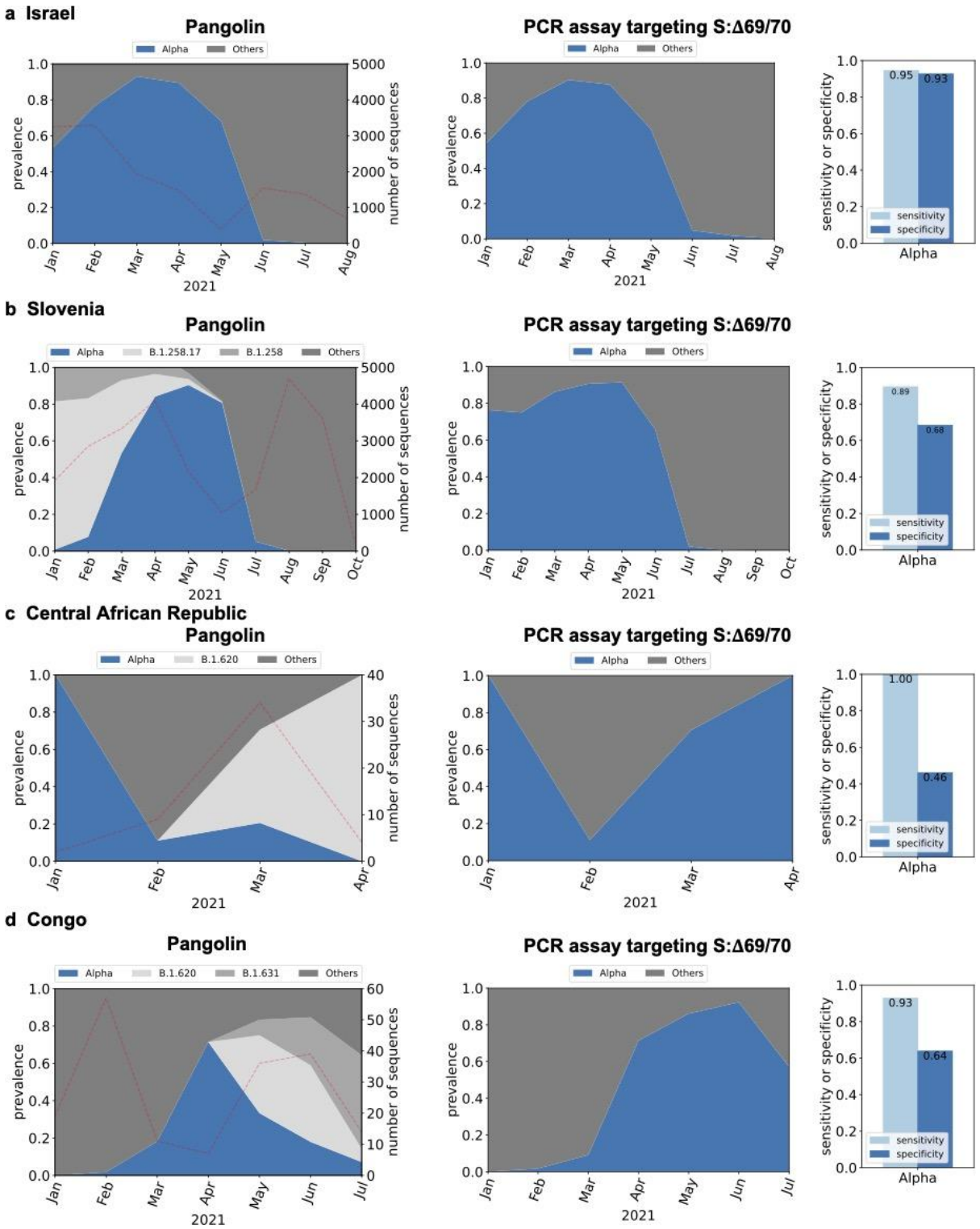

Fig. 2. *In silico* analysis of PCR assay targeting S:Δ69/70 mutation[18] to detect the Alpha variant for GISAID samples from (**a**) Israel (n=13,932), (**b**) Slovenia (n=25,528), (**c**) Central African Republic (n=49) and (**d**) Congo (n=183). Dotted lines on left figures indicate the number of sequences used for the *in silico* analyses.

We conducted a similar analysis for another PCR assay targeting mutation S:Δ144/145 to detect the Alpha variant[13]. This assay was applied to samples from wastewater treatment plants and selected residential buildings across the USA to track the occurrence of the Alpha variant over time in 19 communities. **SI Fig. 1a** shows that this assay works well for GISAID sequences from the USA with estimated sensitivity and specificity of 0.90 and 0.98, respectively. However, several lineages including C.1.2, B.1.620, B.1.1.318, B.1.525 (or the Eta variant), B.1.637, B.1.625, and AZ.2 also have the same mutation S:Δ144/145 targeted by this assay. This PCR assay can produce false results if any of the aforementioned lineages have significant prevalence in the area being studied. For example, we analyzed GISAID sequences collected from Gabon (n=254, from January 2021 to May 2021). **SI Fig. 1b** suggests that Gabon had significant sequences from the Eta variant and the B.1.1.318 lineage from February 2021 to May 2021, both of which have the target mutation S:Δ144/145 mutation. As a result, even though the number of sequences from the Alpha variant increased from February 2021 to April 2021 and then decreased in May 2021, the PCR assay would have predicted a continuous increase in the prevalence of the Alpha variant from February 2021 to May 2021 (**SI Fig. 1b**). The estimated specificity of this assay for detecting the Alpha variant on GISAID sequences from Gabon is only 0.74. We see a similar result by analyzing GISAID sequences from Togo (n=157 from January 2021 to April 2021) in **SI Fig. 1c**. In fact, many countries in Africa, including Nigeria and Ghana, were also expected to have lower specificity for the PCR assay targeting S:Δ144/145 because of B.1.1.338 and B.1.525 lineages (**SI Table 1**).

185 This propensity for false positive results is not limited to PCR assays developed to detect
186 samples from the Alpha variant. We demonstrate this by considering a recent PCR assay targeting
187 mutation S:T478K of the Delta and Delta plus lineages[17]. However, this mutation is also present
188 in the B.1.1.519 lineage. This lineage accounted for only around 1.2% of sequences from the USA
189 (n=1,187,412 from January 2021 to October 2021), so the PCR assay targeting S:T478K was
190 expected to work well for IL, USA, showing 0.94 of estimated sensitivity and 0.97 of estimated
191 specificity (**Fig. 3a**). However, the B.1.1.519 lineage was dominant in Mexico (n=28,956) and
192 explained 30% of the total GISAID sequences from January 2021 to October 2021 (**Fig. 3b**).
193 Therefore, our analysis shows that the PCR assay targeting S:T478K would estimate that the Delta
194 variant was dominant all the way from January 2021 to October 2021, when in reality, Delta variant
195 sequences were collected and later deposited in GISAID, starting May 2021 (**Fig. 3b**).
196
197
198

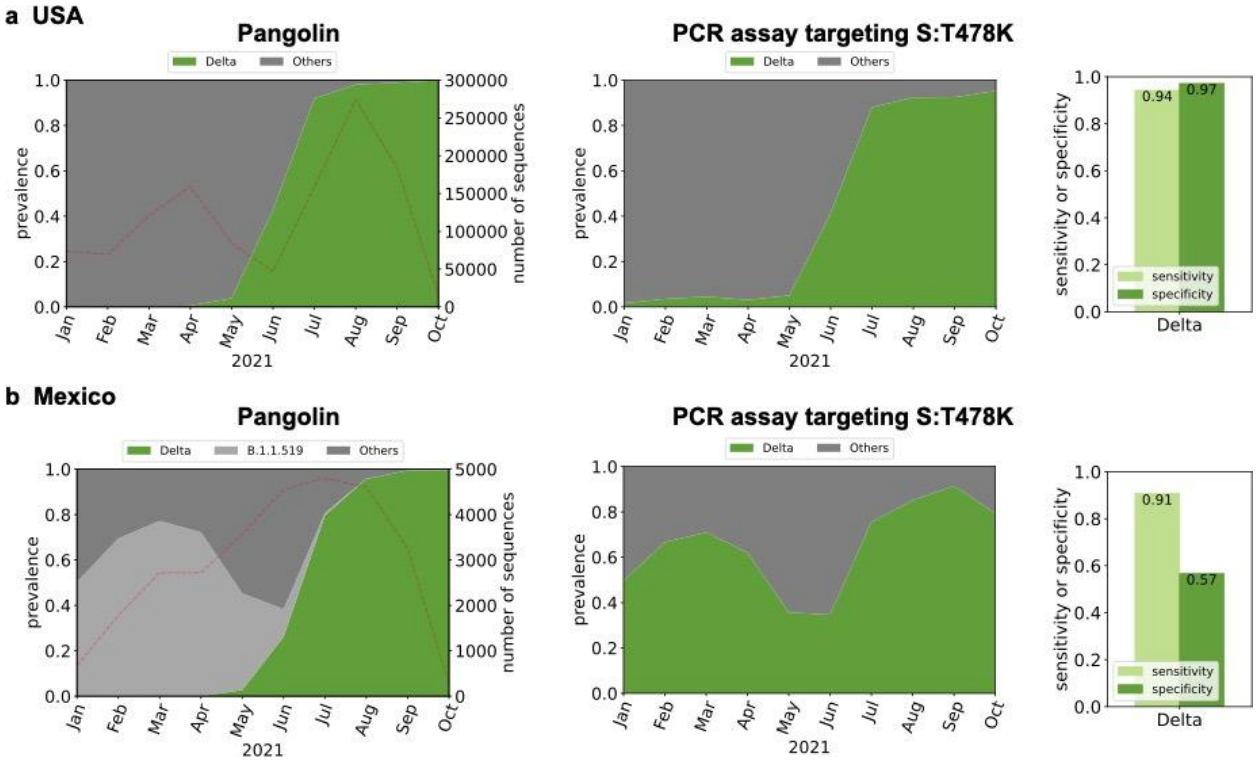

Fig. 3. *In silico* analysis of PCR assay targeting S:T478K mutation[17] to detect the Delta variant: (**a**) USA (n=1,187,412) and (**b**) Mexico (n=28,956). Dotted lines on left figures indicate the number of sequences used for the *in silico* analyses.

The examples of regional and temporal characteristics affecting the accuracy of PCR assays for the detection of SARS-CoV-2 samples of specific lineages of interest are not limited to the cases mentioned above. Globally, only a few VOCs and VOIs accounted for higher than 1% of the total sequences in GISAID, while most of other SARS-CoV-2 lineages explain less than 1%. However, as we examine narrower regions, we may find outbreaks of certain lineages that could be overlooked when we focus on the prevalence on a global scale. For example, as of October 2021, B.1.526 lineage accounted for 1% of reported sequences in the world. However, the prevalence of the lineage increases as we narrow down the study area to local: 4% in the U.S., 17% in New York state, and 30% in Bronx country. In the case of B.1.429 lineage, the prevalences are 1%, 4%, 11%, and 38% in the world, the U.S., California State, and Riverside County,

214 respectively. The number of B.1.258 lineage was less than 0.5% of total sequences worldwide, but
215 it accounted for 54% of cases in Cyprus.

216 We summarized SARS-CoV-2 lineages that have the same mutation that our target variant
217 possesses in **SI Table 1**. When we use PCR assays targeting certain mutations, this table will help
218 identify the lineages that would interfere with our PCR assay. In **SI Table 2**, we also tabulated
219 countries where each of the SARS-CoV-2 lineages summarized in **SI Table 1** accounted for higher
220 than 1% of total sequences. This table will explain whether the lineages that would interfere with
221 your PCR assays are dominant in the study areas. By interpreting **SI Table 1** and **SI Table 2**
222 together, we can find various examples where certain PCR assays would not work reliably. In
223 conclusion, the findings that previously developed PCR assays would not work for certain regions
224 due to the presence of lineages sharing some unique mutations with other lineages motivated us to
225 establish PCR assays for variant detection based on the characteristics of sequences reported from
226 our target study area (IL, USA).

227

228 **Design of variant-specific PCR assays considering regional and temporal characteristics**

229 We describe the proposed workflow to design variant-specific PCR assays considering regional
230 and temporal variant dynamics using `PRIMES` (**Fig. 4a**). Our goal is to design variant-specific
231 PCR assays to track variants with significant prevalence in the USA, with a particular focus on the
232 state of Illinois.

233 First, we investigated the prevalence of SARS-CoV-2 lineages in our regions of interest to
234 select lineages that we need to track. To this end, we downloaded 1,187,412 SARS-CoV-2
235 sequences from GISAID collected between January 2021 and October 2021 in the USA, including
236 20,165 sequences collected in Illinois. These sequences were assigned to the most likely lineage

using Pangolin (**Fig. 4b, e**). Focusing on the variant dynamics in the state of Illinois (**Fig. 4b**), we observe that the B.1.2 lineage was dominant from January (61%) to February (44%), eventually giving way to the Alpha variant. The Alpha variant became dominant in April (44%), May (61%), and June (62%). Then, the Delta variant samples replaced the Alpha variant samples and has been the dominant lineage in the state (95% in July and >99% in August, September and October). Other VOIs and VOCs, including Epsilon, Iota, and Beta variants, accounted only for 2.2%, 1.5%, and 0.4% of total sequences, respectively. Similar trends were observed in sequences collected throughout the USA (**Fig. 4e**). Based on the variant dynamics of our regions of interest, we decided to design PCR assays to enable monitoring of the two major variants, the Alpha and the Delta variants.

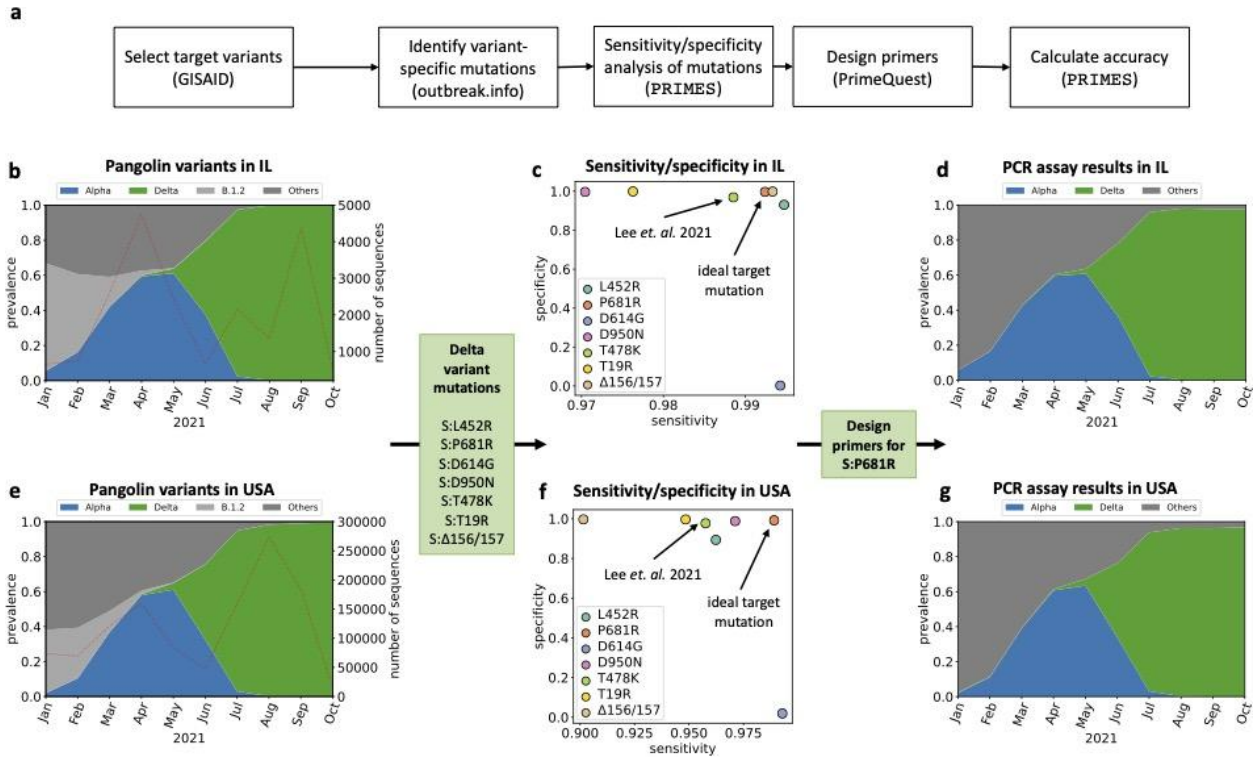

Fig. 4. (**a**) A schematic describing the workflow for designing PCR assays while considering regional and temporal variations in GISAID samples. Variant dynamics determined by Pangolin using GISAID samples from **(b)** the state of Illinois in USA (n=20,165) and (**e**) USA (n=1,187,412). Focusing on the spike protein mutations in the Delta variant, we show the sensitivity and specificity of assigning the Delta variant based on the presence of each mutation in GISAID samples from **(c)** IL and **(f)** USA. The estimated performance on the primer designed to target mutation S:P618R on GISAID samples from **(d)** IL and **(g)** USA.

Second, we designed PCR assays to find unique mutations that are exclusive to our lineage of interest. We utilized https://covariants.org to list up nonsynonymous mutations that define target variants (**SI Table 1**). We focused on mutations located in the spike gene, which has a higher frequency of mutation than other SARS-CoV-2 genes[22]. Previous studies have shown that primers targeting mutations in the spike gene enable accurate detection of SARS-CoV-2 lineages in sewage samples with low virus concentration[21]. As a result, for the Alpha variant, we identify 9 mutations in the spike gene – S:Δ69/70, S:Δ144, S:N510Y, S:A570D, S:D614G, S:P681H, S:T716I, S:S982A, and S:D1118H. For the Delta variant we identify 7 mutations – S:T19R, S:Δ156/157,

265 S:L452R, S:T484K, S:D614G, S:P681R, and S:D950N. Note that mutation S:T484K was targeted
266 by the PCR assay to detect the Delta and Delta plus variant[17].

267 Third, we used `PRIMES` to compute the sensitivity and specificity of lineage assignments
268 performed using each of the selected mutations. We assumed if the specificity and sensitivity of
269 the mutations are higher than 0.99, the mutations are exclusive to the target variant. This criterion
270 allows us to identify the ideal target mutation for the design of the PCR assay that would yield
271 high specificity and sensitivity in our regions of interest. For the Alpha variant, we found three
272 acceptable mutations (S:A570D, S:T716I, and S:S982A) (**SI Fig. 2b**), and we chose the S:A570D
273 mutation because PCR assay targeting S:A570D has already been verified to work for sewage
274 samples, we adopted this mutation in our analysis[13]. For the Delta variant, We found three
275 acceptable mutations (S:L452R, S:P681R, and S:Δ156/157) with GISAID samples from the state
276 of Illinois. However, if we look at all GISAID samples from the USA, the sensitivity for S:L452R
277 and S:Δ156/157 mutations to characterize the Delta variant drops below 0.97. Thus, regional
278 variation can lead to a drastic change in the performance of variant-specific PCR assays. Since our
279 goal is to develop PCR assays that are effective in other states besides Illinois in the USA as well,
280 we instead choose S:P681R, which has high sensitivity and specificity in both Illinois (sensitivity
281 is 0.99 and specificity is 0.99) as well as the USA (sensitivity is 0.99 and specificity is 0.99).
282 Importantly, this mutation has higher sensitivity and specificity in both regions of interest
283 compared to mutation S:T478K (sensitivity is 0.99 and specificity is 0.97 in Illinois, while
284 sensitivity is only 0.96 and specificity is only 0.98 in the USA) that previously targeted to monitor
285 the Delta and Delta plus variants[17].

286 The fourth step is to design the allele-specific primers for the selected mutations. Since
287 both our selected target mutations are single nucleotide polymorphisms (SNPs), we designed

288 allele-specific qPCR assays in which either a forward or a reverse primer target the SNP at the 3'
289 end with a mismatch near the SNP location to improve the specificity of the assays[13]. All RT-
290 qPCR assays were designed using PrimerQuest (Integrated DNA Technologies; IDT, USA) to
291 have an annealing temperature from 58 to 63 °C for primers and GC contents from 30 to 60%.

292 Finally, we estimate the efficacy of the candidate RT-qPCR assays using `PRIMES`.
293 Specifically, we determine the sensitivity and specificity of our assays on the GISAID samples
294 collected from the regions of interest by searching for sequences of a forward primer and a reverse
295 primer in each query sequence. Note that the sequences of reverse primers were converted to
296 reverse sequences to have all sequences, including primers and viruses, on the same strand. If the
297 viral sequence includes the forward and reverse sequences, we assumed that the PCR assay would
298 detect the viral sequence (an illustrative example is shown in **SI Fig. 3**). We note that operational
299 failures of the assay due to inappropriate primer design or PCR inhibitors are not considered by
300 `PRIMES`. Some lineages should be expected to lower the sensitivity or specificity of our assays
301 based on **SI Table 1** (e.g., B.1.1.189, C38, and B.1.636 for the Alpha variant detection and AU.3,
302 AU.2, P.1.8, B.1.617.3, A.23.1, B.1.617.1, B.1.551, B.1.466.2, B.1.1.528, Q.4, B.1.623, B.1.1.25,
303 C.36, and AY.28 for the Delta variant detection), but importantly those lineages were not detected
304 or had very low prevalence in our regions of interest. The estimated sensitivity and specificity for
305 PCR assays designed to detect viruses from the Alpha and Delta variants were all high for our
306 study scope, and in Illinois in particular (sensitivity is 0.99 and specificity is 0.99 for detection of
307 Alpha variant and sensitivity is 0.98 and specificity is 1.00 for detection of the Delta variant in
308 Illinois, see **SI Fig. 4** for sensitivity and specificity of detecting the two variants in GISAID
309 samples from all of the USA). These values are higher than the sensitivity and specificity estimated
310 for the previously developed PCR assays in their regions of interest (see **Fig. 1, 2** and **3**). In the

311 subsequent section, we demonstrate this performance of our PCR assays translated to synthetic
312 controls and actual sewage samples collected in our community.
313
314 **Verification of PRIMES-designed PCR assays by synthetic RNA controls**
315 We applied the RT-qPCR assays designed with PRIMES to synthetic RNA controls for
316 WT, Alpha, and Delta variants to experimentally confirm the sensitivity (i.e., the limit of
317 quantification; LOQ and limit of detection; LOD) and specificity (i.e., cross-reactivity). Regarding
318 sensitivity, we found that the LOQs for total SARS-CoV-2, Alpha variant, and Delta variant were
319 all 10 gene copies (gc)/μL or 50, 30, and 30 gc/reaction, respectively (**SI Fig. 5a**). Also, the LODs
320 of RT-qPCR assays for total SARS-CoV-2, Alpha variant, and Delta variant were 1.0, 1.3, and 1.3
321 gc/μL or 5.0, 3.9, and 3.8 gc/reaction, respectively (**SI Fig. 5b**). Because LODs for our assays
322 were close to the theoretical LODs of RT-qPCR (3.0 gc/reaction)[23], we concluded that our RT-
323 qPCR assays are sensitive to detect RNA of target variants.
324 As for the cross-reactivity, we found that when the concentrations of the RNA synthetic
325 control were high (i.e., 10^4 and 10^5 gc/μL), we detected Cq values from WT RNA controls. This
326 finding suggests that the presence of WT caused false positives for the Alpha variant detection
327 (**SI Fig. 6a**). However, the Cq value differences between the Alpha variant and WT were greater
328 than 11 that is about 10^3-fold difference in RNA concentrations. This difference in Cq values is
329 equivalent to less than 0.1% error when quantifying the Alpha variant, and thus we considered this
330 error is acceptable for our study. When the RNA synthetic control concentrations were low (i.e.,
331 less than 10^3 gc/μL), the Cq values from WT were lower than LOD, which will be disregarded in
332 this study, so the false positives were not detected. We found similar results from the specificity
333 experiments for the Delta variant assay (**SI Fig. 6b**). When the concentrations of the RNA synthetic

334 controls were high (i.e., 10^4 and 10^5 gc/μL), the Cq value differences from Delta variant and WT
335 were greater than 13. At the lower concentration (i.e., less than 10^3 gc/μL), the Cq values from
336 WT (i.e., false positives) were less than LOD. Because the measured cross-reactivities by WT were
337 negligible, we concluded our RT-qPCR assays are specific to measure target variants.

338 We further confirmed the applicability of PRIMES-designed PCR assay to determine
339 predominant variants in mixtures of synthetic RNA controls. The results from the mixtures of
340 synthetic RNA controls are presented in **Fig. 5a** and **5b**. The y-axis shows the prevalences, which
341 are the ratios of each variant's concentration to total SARS-CoV-2 concentration. The variant
342 showing the highest prevalence became the dominant variant. If none of the two targets (i.e., Alpha
343 and Delta variants) are higher than 0.5, the Others, which indicate all SARS-CoV-2 lineages other
344 than our target variants (i.e., the Alpha and Delta variant), became the dominant variant. With the
345 highest total virus concentrations (10^4 gc/μL), our RT-qPCR assays successfully assign the correct
346 dominant variant to all experimental cases ($p < 0.001$) (**Fig. 5a**). For example, in the case of the
347 mixtures between WT and Alpha variant, we assigned Alpha variant to the RNA mixtures whose
348 actual prevalence of Alpha variant were 0.7 and 0.9 whereas we assigned 'Others' when the
349 prevalence of Alpha variant were 0.1 and 0.3. In the same manner, we also assigned the dominant
350 variant correctly to the mixtures of Alpha and Delta variants. Specifically, we assigned the Alpha
351 variant when the actual prevalences of Alpha variant were 0.7 and 0.9. At the same time, the Delta
352 variant was assigned to the other two mixtures whose prevalences of Alpha variant were 0.1 and
353 0.3. In addition, we found that the PCR assays assigned the dominant variant correctly when the
354 total virus concentrations were 10^1 gc/μL for all mixing ratios (**Fig. 5b**). However, the statistical
355 analysis showed that the comparisons of prevalences determined by the RT-qPCR were significant
356 only when the mixing ratios were 0.9:0.1 or vice versa for mixtures of WT and Alpha variant or

357 Alpha variant and Delta variant. Note that when total virus concentrations were 10^1 gc/μL,
358 concentrations of each synthetic RNA control were ranging from 1×10^0 to 9×10^0 gc/μL depending
359 on the mixing ratios, which were less than their LOQs (10^1 gc/μL). Based on these findings, we
360 concluded that our RT-qPCR assays could find the dominant variant when total SARS-CoV-2
361 concentrations are higher than LOQs (10^1 gc/μL) and the prevalence of target variants is higher
362 than 0.9 (**Fig. 5b**). When the total SARS-CoV-2 concentrations become higher, Alpha and Delta
363 variant concentrations are higher than LOQs of the RT-qPCR assays (10^1 gc/μL), our RT-qPCR
364 assays can assign the dominant variant when its prevalence is higher than 0.7 (**Fig. 5a**).
365
366

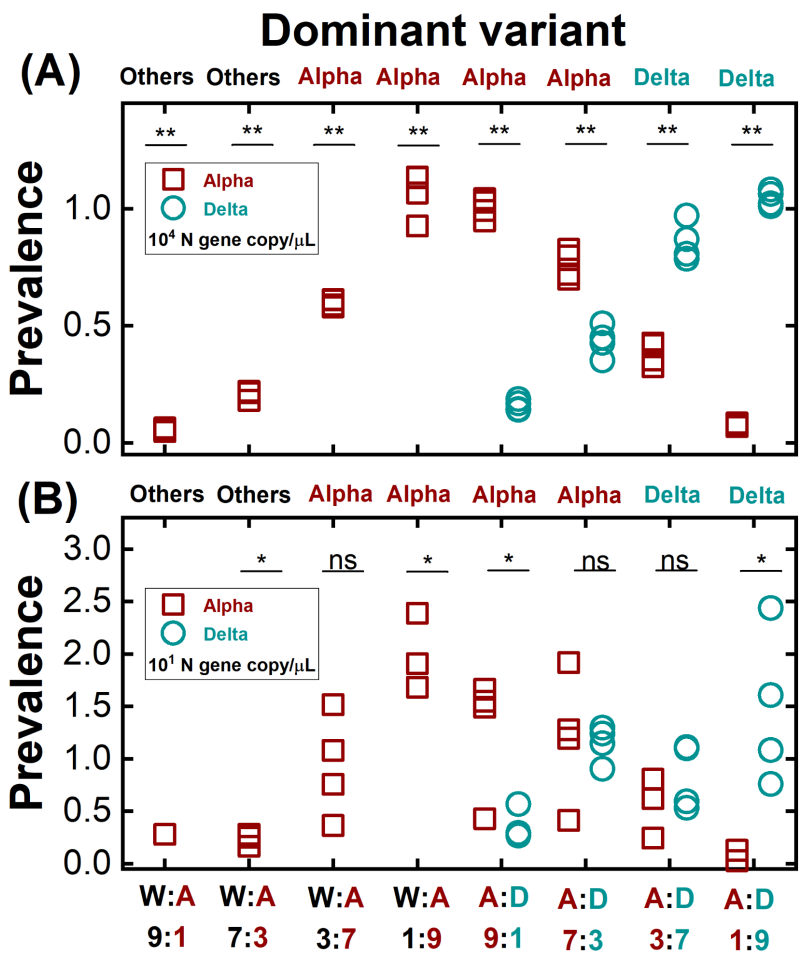

Fig. 5. The dominant variants of the mixtures of synthetic RNA controls determined by RT-qPCR assays. Total SARS-CoV-2 concentrations were determined by the N gene concentrations at **(a)** 10^4 gc/μL and **(b)** 10^1 gc/μL. Prevalences on the y-axis indicate the ratio of each variant' concentration to the total virus concentrations. The x-axis presented the mixing ratios of different synthetic RNA controls (W, A, and D stand for WT, Alpha variant and Delta variant, respectively). Decisions made on top of each graph showed the dominant variant determined by the RT-qPCR assays. One sample t-test or two-sample t-test were conducted to compare prevalence between Alpha variant and 0.5 or the prevalences between Alpha and Delta variants (ns: $p>0.05$, *: $0.001<p<0.05$, **:$p<0.001$), respectively.

Application of PCR assays to sewage samples and confirmation by NGS

We applied our PCR assays to six different local sewage samples. We first obtained RNA extracts from those sewage samples. The total SARS-CoV-2 concentrations (i.e., N gene) of these RNA extracts ranged from 1.4×10^1 to 1.8×10^2gc/μL (**SI Table 3**). After accounting for

382 recovery efficiencies and concentration factors, the SARS-CoV-2 concentrations (i.e., N gene) of
383 these sewage samples ranged from 1.3×10^3 to 6.0×10^4 gc/L (**Eq. 3**). These concentrations
384 agree with the SARS-CoV-2 concentrations of sewage samples analyzed previously [24]. Then, we
385 determined the prevalence of variants based on the ratios of the Alpha variant concentration
386 (determined by PRIMES-designed PCR) over the total SARS-CoV-2 (N gene). We found that
387 sample #1 has 0.85 prevalence of the Alpha variant. Based on the results with the RNA synthetic
388 mixtures, we assigned the Alpha variant as a dominant variant to sample #1. Similarly, we
389 assigned the Delta variant to Sample #5 and #6 because of their prevalences of 0.92 and 0.73,
390 respectively. On the other hand, none of the Alpha and Delta variants presented higher than 0.5
391 prevalence for Sample #2, #3, and #4, so we assigned Others to these three samples.

392 To further confirm whether the RT-qPCR results were correct, we conducted NGS analysis
393 to examine eight mutation markers for the Alpha variant (S:Δ69/70, S:Δ144, S:N501Y, S:A570D,
394 S:P681H, S:T716I, S:S982A, and S:D1118H) and six mutation markers for the Delta variant
395 (S:T19R, S:Δ156/157, S:L452R, S:T478K, S:P681R, and S:D950N) on the spike gene of two
396 sewage samples (#5 and 6) and three synthetic RNA controls (WT, Alpha, and Delta variant).
397 Samples #1, #2, #3, and #4 were not appropriate for sequencing due to the low SARS-CoV-2
398 concentrations ($<10^2$ gc/μL). From Sample #5 and #6 classified to the Delta variant by the RT-
399 qPCR assays, we detected all six mutations for the Delta variant. In comparison, none of the eight
400 mutations for the Alpha variant were detected in these samples. We believe the NGS analyses were
401 reliable because of the results with the synthetic RNA controls. We detected all mutation markers
402 with corresponding synthetic RNA controls. For example, we detected the eight Alpha variant
403 mutations from the Alpha variant RNA samples and found the six Delta variant mutations from
404 Delta variant RNA controls (**Table 1**). Therefore, the agreement between the NGS analysis and

405 RT-qPCR assays supports that our RT-qPCR can assign the most likely variant for the local sewage
406 samples.
407
408 **Table 1.** Comparisons between RT-qPCR assays and NGS analysis

Sample	Mutation markers for Alpha variant								Mutation markers for Delta variant					
	Δ69/70	Δ144	N501Y	A570D	P681H	T716I	S982A	D1118H	T19R	Δ156/157	L452R	T478K	P681R	D950N
RNA for WT														
RNA for Alpha variant														
RNA for Delta variant														
Sewage #5														
Sewage #6														

409 1) Orange color represents that mutations are detected while gray color indicates that
410 mutations are not detected.
411

412 ## Discussion

413 PCR assays have advantages for SARS-CoV-2 variant detection in sewage over sequencing
414 technologies such as low cost, fast turnaround, and robustness to environmental samples.
415 However, PCR assays can examine only a few mutations due to size constraints of primer and
416 probe sequences, compromising their accuracy as distinct SARS-CoV-2 lineages may share target
417 mutations. We used the `PRIMES` algorithm to show that the current variant-specific PCR assays
418 have diminished accuracy when applied outside the region where they were developed. These
419 findings suggest that considering regional and temporal dynamics of variants is important to secure
420 the sensitivity and specificity of PCR assays that target only a limited number of mutations.
421 Subsequently, we used `PRIMES` and open-source databases (e.g., GISAID, Pangolin, or

422 outbreak.info) to design PCR primers to determine the dominant SARS-CoV-2 variants (i.e.,
423 Alpha and Delta variant) in local sewage samples.

424 The regional and temporal variations are especially critical for SARS-CoV-2 detection
425 because various SARS-CoV-2 lineages with different genotypes have been reported across the
426 world. Commercial PCR kits for variant detection are currently available. However, these kits also
427 target a few mutation markers originating from SARS-CoV-2 lineages of interest[25–27]. As we
428 showed above, targeting a single mutation could make the assay less accurate at certain regions
429 due to the presence of other lineages that have the same mutation. In addition, our findings are not
430 limited to PCR assays, but are also relevant for the other types of molecular assays such as loop-
431 mediated isothermal amplification (LAMP), PfAgo-based assay, and Clustered, Regularly-
432 Interspaced Short Palindromic Repeats (CRISPR)-based assays that are designed to detect specific
433 RNA sequences for virus detection[28–30]. For example, two LAMP assays that target N genes for
434 SARS-CoV-2 test could have low accuracy when applied outside of Germany or the US, where
435 the assays were developed and verified with clinical samples[28,31]. This low accuracy issue could
436 happen because their primers include sequences for N:A119S, a mutation marker for the Zeta
437 variant (P.2 lineage). The Zeta variant was dominant in some South American countries
438 (Suriname, Paraguay, Uruguay, and Brazil). Zhang et al. (2021)[32] designed a LAMP assay
439 targeting the ORF1a gene, but their F2 primer includes sequences for ORF1a:V86F and F1 primer
440 ORF1:E102K. The Food and Drug Administration (FDA) also recommended that mutations
441 present in the sequences where molecular diagnostic tests target for virus detection should be
442 monitored by *in silico* analysis[33]. Our `PRIMES` tool allows users and developers of molecular
443 diagnostic assays to follow this recommendation.

444 Perfect loci to target viral mutation are not realistic because viruses evolve randomly, so
445 one that looks perfect could be affected by emerging variants. For example, the S:Δ69/70 mutation
446 used to be a unique mutation for the Alpha variant, but the Eta variant, which appeared later, also
447 has the same mutation. Thus, if the S:Δ69/70 is considered an exclusive mutation to the Alpha
448 variant, the Eta variant will be false positive for the Alpha variant. In addition, sub-lineages in the
449 target variant may not have one of the mutation markers for the target variant. For example, less
450 than 0.5% of Q.4 (one of the sub-lineages for the Alpha variant and reported December 2020) is
451 known to have a S:P681H. The S:P681H mutation is one of the mutation markers for the Alpha
452 variant. Thus, if S:P681H mutation is targeted for the Alpha variant, Q.4 will cause false negatives.
453 These examples demonstrate that PCR assays could have different sensitivities and specificities
454 depending on various lineages of SARS-CoV-2 that coexist with the target lineage.
455 Global genomic databases for emergent variants have greatly improved since the onset of
456 COVID-19 pandemics[34]. Before COVID-19, influenza sequences are archived in GISAID. Fast
457 mutating pathogens such as influenza and coronavirus should be monitored because they have
458 pandemic potential. As we showed in this study, assays targeting these pathogens need to keep up
459 with their evolution, and the developed methodology facilitates genomic surveillance of any fast
460 mutating pathogen.
461

462 ## Online Methods

463 **Sewage samples**

464 We followed the Minimum information Environmental Microbiology Minimum Information
465 (MIQE) Guidelines to ensure the credibility and reproducibility of our data[35]. Detailed information
466 on the MIQE is summarized in **SI Table 4**. Also, detailed information from sample collection to

467 data analysis is described in **SI Table 5**. Briefly, we used ISCO automatic samplers (6712 ISCO,
468 Teledyne ISCO, USA) to collect three-day composite sewages (about 2 L) from the sewer
469 distribution system across Champaign County, IL, USA. $MgCl_2$ was added to the sewage samples
470 at the final concentration of 50 mM to facilitate the coagulation of viruses and sewage sludge. We
471 kept sewage samples on ice while moving them to our laboratory in 2 hours. We gently removed
472 the supernatant upon arrival and added 200 µL of bovine coronavirus (BCoV) to the remaining
473 solution (about 50 mL) to determine virus recovery efficiency. After 5 minutes of incubation at
474 room temperature, we centrifuged the mixture at 10,000 rpm (13,900 g) for 30 minutes (Sorvall
475 Legend RT Plus, Thermo Fisher Scientific, USA). The supernatant was discarded again, and the
476 sludge (about 1 g) was taken to harvest viruses. Then, we extracted viral RNA from the sludge
477 using the Viral RNA extraction Mini Kit (Qiagen, Germany) following the manufacturer's
478 procedure. The RNA extracts were purified using an RNA purification kit (RNeasy MinElute
479 Cleanup Kit, Qiagen, German) to reduce the PCR inhibitions. It took less than 9 hours from sample
480 collection to RNA extraction. The RNA samples were stored at -80°C until downstream analyses
481 were ready. The same sample preparation processes were applied to drainages discharged from a
482 food processing industry whenever we processed sewage samples. There are no sources of human
483 feces that merged to these drainages, which were therefore used for negative controls. Indeed, we
484 did not detect any SARS-CoV-2 from these negative controls. Therefore, we are confident there
485 were no false positives for SARS-CoV-2 in our sewage samples. With the concentrations of RNA
486 extracts, we used Eqs. 3-5 to determine the virus concentrations in sewage samples.
487

488 $$C_{Sewage}\ (gc/L) = C_{RNA\ extract}\ (gc/\mu L) \times \frac{Concentration\ factor\ (\mu L/L)}{Recovery\ efficiency} \quad \text{(Eq. 3)}$$

489 $$Concentration\ factor\ (\mu L/L) = \frac{Volume\ of\ RNA\ extract\ (\mu L)}{Volume\ of\ initial\ sewage\ (L)} \quad \text{(Eq. 4)}$$

490 $$Recovery\ efficiency = \frac{The\ number\ of\ BCoV\ in\ RNA\ extract}{The\ number\ of\ BCoV\ in\ initial\ sewage}$$ (Eq. 5)

491

492 **Determination of LODs and LOQs**

493 We first determined the limit of detection (LOD) and the limit of quantification (LOQ) for
494 Alpha and Delta variants with serial dilutions of the synthetic RNA controls. We prepared 10-fold
495 serial dilutions of synthetic RNA controls and determined a positive sample fraction at each
496 concentration. The number of replicates for concentrations near LOD are 20 while the sample
497 numbers for the higher concentration were 4. We used a sigmoidal function (**Eq. 6)** to determine
498 the trend lines for fraction positive samples with different concentrations and calculated the LODs
499 [36].

500

501 $$Y = \frac{1}{1+e^{-a-b\times log(X)}}$$ (Eq. 6)

502

503 where X is gene copy (gc/μL), Y means positive rate, and both a and b are constants. LOQ was
504 defined as the lowest concentration with coefficient of variation (CV) less than 35%[36]. We
505 calculated CV by **Eq. 7**.

506

507 $$CV = \sqrt{(1+E)^{(SD)^2\times ln(1+E)} - 1}$$ (Eq. 7)

508

509 where E is a qPCR efficiency, SD is a standard deviation of Cq values.

510

511 **PCR assays for SARS-CoV-2 variant detection in synthetic RNA control**

512 We applied the RT-qPCR assays to 10-fold serial dilutions of synthetic RNA controls to determine
513 LOQs and LODs. LOQ was defined as the lowest concentration with coefficient of variation (CV)
514 less than 35%[36] and LOD was defined as the concentration at which RNA samples test positive
515 (i.e., Cq<40) with 95% probability. For example, we applied the RT-qPCR assay for Alpha variant
516 to 10-fold serial dilutions of Alpha variant RNA controls and those of the WT RNA controls, then
517 compared the Cq values from Alpha variant and WT.

518 We applied each of RT-qPCR assays for Alpha and Delta variant to the synthetic controls
519 of its target variant and WT to determine the cross-reactivity. This process is important because
520 our assays for the Alpha and Delta variants were designed to detect only a SNP of target variants
521 among other lineages that do not have the same SNP. In this experiment, we mixed synthetic RNA
522 controls of WT and Alpha variant or Alpha and Delta variant because these two mixtures
523 represented the transitions where one dominant variant was replaced by the other one in our
524 community. For instance, the Others (mainly B.1.2) were dominant until February 2021 and the
525 Alpha variant raced for the dominant variant in around March 2021. Also, the Alpha variant was
526 dominant from April and May in 2021, but the Delta variants competed with the Alpha variant in
527 around June 2021 (**Fig. 4b**). Total SARS-CoV-2 concentrations (i.e., N gene concentrations) of
528 the mixtures were 10^4 and 10^1 gc/μL, which are the reasonable concentration range of SARS-CoV-
529 2 of local sewage samples[24]. Also, we mixed the two different RNA controls with four different
530 ratios (i.e., 9:1, 7:3, 3:7, and 1:9) to mimic different scenarios of variant dynamics.

531

532 **PCR assays for SARS-CoV-2 variant detection in sewage samples**

533 We conducted six different RT-qPCR assays to analyze sewage samples. Three of them targeted
534 different loci of SARS-CoV-2 genome for virus quantification and the dominant variant detection.
535 The other three assays were applied to measure bovine coronavirus (BCoV), pepper mild mottle
536 virus (PMMoV), and Tulane virus (TV), which were used for calculation of virus recovery
537 efficiency, normalization of SARS-CoV-2 to human feces, and inhibition tests, respectively. 2-
538 fold diluted the RNA samples in molecular biology grade water (Milliporesigma, USA) before the
539 quantification. We used Taqman-based RT-qPCR for the N1 gene detection as suggested by CDC
540 and SYBR-based RT-qPCR for the other six assays (**SI Table 6**). The SYBR-based RT-qPCR
541 started with mixing the 3 μL of viral genome with 5 μL of 2 × iTaq universal SYBR green reaction
542 mix, 0.125 μL of iScript reverse transcriptase from the iTaq universal SYBR green reaction mix
543 (Bio-Rad Laboratories, USA), 0.3 μL of 10 μM forward primer for each virus, 0.3 μL of 10 μM
544 reverse primer for each virus, and 1.275 μL of molecular biology grade water (Corning, NY, USA).
545 The PCR cocktail for the one-step RT-qPCR was placed in 96-well plates (4306737, Applied
546 Biosystems, USA) and analyzed by a qPCR system (QuantStudio 3, Thermo Fisher Scientific,
547 USA). The thermocycle began with 10 minutes at 50°C and 1 minute at 90°C followed by 40 cycles
548 of 30 seconds at 60°C and 1 minute at 90°C. The Taqman-based RT-qPCR was initiated by mixing
549 5 μL of viral genome with 5 μL of Taqman Fast Virus 1-step Master Mix (4444432, Applied
550 Biosystems, USA), 1.5 μL of primers/probe mixture for N1 gene (2019-nCoV RUO kit, Integrated
551 DNA Technologies, USA), and 8.5 μL of water. The 20 μL of mixture was analyzed by the same
552 qPCR system as used for the SYBR-based RT-qPCR, except for a different thermal cycle (5
553 minutes at 50°C, 20 seconds at 95°C followed by 45 cycles of 3 seconds at 95°C and 30 seconds
554 at 55°C). We used synthetic RNA controls to get standard curves for WT, Alpha variant, and Delta

555 variant (TWIST Bioscience, USA, Part numbers are 102024, 103907, and 104533, respectively).
556 The PCR standard curves were obtained for every RT-qPCR analysis with 10-fold serial dilutions
557 of synthetic RNA controls and PCR efficiencies for RT-qPCR were higher than 85% (R^2>0.99).
558 The SYBR signal was normalized to the ROX reference dye. The cycle of quantification (Cq)
559 values was determined automatically by QuantStudio™ Design & Analysis Software (v1.5.1).
560 Based on the melting curves, the primers were specifically bound to the target genome. The
561 numbers of technical replicates were 4 for synthetic RNA controls and 3 for sewage samples except
562 for LODs and LOQs determination where 20 replicates were analyzed.
563

564 **Next-generation sequencing to assign SARS-CoV-2 lineages**

565 The PCR results were confirmed by sequencing the spike gene of three controls (wild type, alpha
566 variant, delta variant) and two sewage samples (#5 and #6) were performed on Illumina MiSeq
567 platform. A set of four pairs of primers in-house designed were used to amplify the spike of RNA
568 samples using SuperScript™ III One-Step RT-PCR System with Platinum™ Taq High Fidelity
569 DNA Polymerase (ThermoFisher). Amplicons were purified using QIAquick PCR Purification Kit
570 (Qiagen), quantified using Qubit fluorometer, and subject to library preparation using Nextera XT
571 kit and sequencing on MiSeq.
572

573 ## Acknowledgment

574 We acknowledge the funding from the Grainger College of Engineering and the JUMP-ARCHES
575 program of OSF Healthcare in conjunction with the University of Illinois. Sequencing was funded
576 in part by the Food and Drug Administration Veterinary Laboratory Investigation and Response
577 Network (FOA PAR-17-141) under grant 1U18FD006673-01. M.E-K. acknowledges the National

Science Foundation (grants: CCF-2027669 and CCF-2046488). The authors also acknoweldge Bill Brown for sampling site selection, Hayden Wennerdahl, Kip Stevenson, and Dr. Schmidt for sampling deployment, and Yuqing Mao, Matthew Robert Loula, Aashna Patra, Kristin Joy Anderson, Mikayla Diedrick, Hubert Lyu, Hamza Elmahi Mohamed, Jad R Karajeh, Runsen Ning, Rui Fu, Kate O'Brien, Nathan Kim for sewage sampling and processing.

585 **Reference**

586 1. Harvey, W. T. *et al.* SARS-CoV-2 variants, spike mutations and immune escape. *Nat.*
587 *Rev. Microbiol. 2021 197* **19**, 409–424 (2021).

588 2. I, L., V, P., D, M. & M, C. Immune Evasion of SARS-CoV-2 Emerging Variants: What
589 Have We Learnt So Far? *Viruses* **13**, (2021).

590 3. Grubaugh, N. D., Hodcroft, E. B., Fauver, J. R., Phelan, A. L. & Cevik, M. Public health
591 actions to control new SARS-CoV-2 variants. *Cell* **184**, 1127–1132 (2021).

592 4. Peccia, J. *et al.* Measurement of SARS-CoV-2 RNA in wastewater tracks community
593 infection dynamics. *Nat. Biotechnol. 2020 3810* **38**, 1164–1167 (2020).

594 5. Larsen, D. A. & Wigginton, K. R. Tracking COVID-19 with wastewater. *Nat. Biotechnol.*
595 *2020 3810* **38**, 1151–1153 (2020).

596 6. Ahmed, W. *et al.* First confirmed detection of SARS-CoV-2 in untreated wastewater in
597 Australia: A proof of concept for the wastewater surveillance of COVID-19 in the
598 community. *Sci. Total Environ.* **728**, 138764 (2020).

599 7. Prado, T. *et al.* Wastewater-based epidemiology as a useful tool to track SARS-CoV-2 and
600 support public health policies at municipal level in Brazil. *Water Res.* **191**, 116810 (2021).

601 8. Gonzalez, R. *et al.* COVID-19 surveillance in Southeastern Virginia using wastewater-
602 based epidemiology. *Water Res.* **186**, 116296 (2020).

603 9. Saththasivam, J. *et al.* COVID-19 (SARS-CoV-2) outbreak monitoring using wastewater-
604 based epidemiology in Qatar. *Sci. Total Environ.* **774**, 145608 (2021).

605 10. Hart, O. E. & Halden, R. U. Computational analysis of SARS-CoV-2/COVID-19
606 surveillance by wastewater-based epidemiology locally and globally: Feasibility,
607 economy, opportunities and challenges. *Sci. Total Environ.* **730**, 138875 (2020).

608 11. Wang, H. *et al.* Multiplex SARS-CoV-2 Genotyping Reverse Transcriptase PCR for
609 Population-Level Variant Screening and Epidemiologic Surveillance. *J. Clin. Microbiol.*
610 **59**, (2021).
611 12. Guglielmi, G. The explosion of new coronavirus tests that could help to end the pandemic.
612 *Nature* **583**, 506–509 (2020).
613 13. Lin Lee, W. *et al.* Quantitative SARS-CoV-2 Alpha Variant B.1.1.7 Tracking in
614 Wastewater by Allele-Specific RT-qPCR. *Cite This Environ. Sci. Technol. Lett* **8**, 675–
615 682 (2021).
616 14. CoVariants. https://covariants.org/.
617 15. Shu, Y. & McCauley, J. GISAID: Global initiative on sharing all influenza data – from
618 vision to reality. *Eurosurveillance* **22**, 30494 (2017).
619 16. Elbe, S. & Buckland-Merrett, G. Data, disease and diplomacy: GISAID's innovative
620 contribution to global health. *Glob. Challenges* **1**, 33–46 (2017).
621 17. Lin Lee, W. *et al.* Quantitative SARS-CoV-2 tracking of variants Delta, Delta plus, Kappa
622 and Beta in wastewater by allele-specific RT-qPCR. doi:10.1101/2021.08.03.21261298.
623 18. Yaniv, K. *et al.* Direct RT-qPCR assay for SARS-CoV-2 variants of concern (Alpha,
624 B.1.1.7 and Beta, B.1.351) detection and quantification in wastewater. *Environ. Res.* **201**,
625 111653 (2021).
626 19. O'Toole, Á. *et al.* Tracking the international spread of SARS-CoV-2 lineages B.1.1.7 and
627 B.1.351/501Y-V2. *Wellcome Open Res. 2021 6121* **6**, 121 (2021).
628 20. Li, H. Minimap2: pairwise alignment for nucleotide sequences. *Bioinformatics* **34**, 3094–
629 3100 (2018).
630 21. Carcereny, A. *et al.* Monitoring Emergence of the SARS-CoV-2 B.1.1.7 Variant through

631 the Spanish National SARS-CoV-2 Wastewater Surveillance System (VATar COVID-19).
632 *Cite This Environ. Sci. Technol* **55**, 11756–11766 (2021).
633 22. Li, Q. *et al.* The Impact of Mutations in SARS-CoV-2 Spike on Viral Infectivity and
634 Antigenicity. *Cell* **182**, 1284-1294.e9 (2020).
635 23. Ståhlberg, A. & Kubista, M. The workflow of single-cell expression profiling using
636 quantitative real-time PCR. *https://doi.org/10.1586/14737159.2014.901154* **14**, 323–331
637 (2014).
638 24. Pecson, B. M. *et al.* Reproducibility and sensitivity of 36 methods to quantify the SARS-
639 CoV-2 genetic signal in raw wastewater: findings from an interlaboratory methods
640 evaluation in the U.S. *Environ. Sci. Water Res. Technol.* (2021) doi:10.1039/d0ew00946f.
641 25. Caza, M. *et al.* Evaluation of the clinical and analytical performance of the Seegene
642 allplex^{TM} SARS-CoV-2 variants I assay for the detection of variants of concern (VOC)
643 and variants of interests (VOI). *J. Clin. Virol.* **144**, 104996 (2021).
644 26. Chan, C. T.-M. *et al.* A low-cost TaqMan minor groove binder probe-based one-step RT-
645 qPCR assay for rapid identification of N501Y variants of SARS-CoV-2. *J. Virol. Methods*
646 **299**, 114333 (2022).
647 27. Hirotsu, Y. & Omata, M. Detection of R.1 lineage severe acute respiratory syndrome
648 coronavirus 2 (SARS-CoV-2) with spike protein W152L/E484K/G769V mutations in
649 Japan. *PLOS Pathog.* **17**, e1009619 (2021).
650 28. Ganguli, A. *et al.* Rapid Isothermal Amplification and Portable Detection System for
651 SARS-CoV-2. *PNAS* 1–9 (2020) doi:10.1101/2020.05.21.108381.
652 29. Broughton, J. P. *et al.* CRISPR–Cas12-based detection of SARS-CoV-2. *Nat. Biotechnol.*
653 *2020 387* **38**, 870–874 (2020).

654 30. Xun, G., Lane, S. T., Petrov, V. A., Pepa, B. E. & Zhao, H. A rapid, accurate, scalable,
655 and portable testing system for COVID-19 diagnosis. *Nat. Commun. 2021 121* **12**, 1–9
656 (2021).
657 31. Thi, V. L. D. *et al.* A colorimetric RT-LAMP assay and LAMP-sequencing for detecting
658 SARS-CoV-2 RNA in clinical samples. *Sci. Transl. Med.* **12**, (2020).
659 32. Zhang, Y. *et al.* Rapid Molecular Detection of SARS-CoV-2 (COVID-19) Virus RNA
660 Using Colorimetric LAMP. doi:10.1101/2020.02.26.20028373.
661 33. Genetic Variants of SARS-CoV-2 May Lead to False Negative Results with Molecular
662 Tests for Detection of SARS-CoV-2 - Letter to Clinical Laboratory Staff and Health Care
663 Providers | FDA. https://www.fda.gov/medical-devices/letters-health-care-
664 providers/genetic-variants-sars-cov-2-may-lead-false-negative-results-molecular-tests-
665 detection-sars-cov-2.
666 34. Maier, W. *et al.* Ready-to-use public infrastructure for global SARS-CoV-2 monitoring.
667 *Nat. Biotechnol. 2021 3910* **39**, 1178–1179 (2021).
668 35. Bustin, S. A. *et al.* The MIQE guidelines: Minimum information for publication of
669 quantitative real-time PCR experiments. *Clin. Chem.* **55**, 611–622 (2009).
670 36. Forootan, A. *et al.* Methods to determine limit of detection and limit of quantification in
671 quantitative real-time PCR (qPCR). *Biomol. Detect. Quantif.* **12**, 1–6 (2017).
672